THE JOURNAL OF BIOLOGICAL CHEMISTRY
Vol. 271, No. 33, Issue of August 16, pp. 19950–19956, 1996

Printed in U.S.A.

Human Phagocytes Employ the Myeloperoxidase-Hydrogen Peroxide System to Synthesize Dityrosine, Trityrosine, Pulcherosine, and Isodityrosine by a Tyrosyl Radical-dependent Pathway*

(Received for publication, December 15, 1995, and in revised form, May 8, 1996)

Jason S. Jacob‡, David P. Cistola§¶, Fong Fu Hsu‡, Samar Muzaffar‡, Dianne M. Mueller‡, Stanley L. Hazen‡‖, and Jay W. Heinecke‡‡‡**

*From the Departments of ‡Medicine, §Biochemistry and Molecular Biophysics, and **Molecular Biology and Pharmacology, Washington University School of Medicine, St. Louis, Missouri 63110*

Myeloperoxidase, a heme protein secreted by activated phagocytes, may be a catalyst for lipoprotein oxidation *in vivo*. Active myeloperoxidase is a component of human atherosclerotic lesions, and atherosclerotic tissue exhibits selective enrichment of protein dityrosine cross-links, a well characterized product of myeloperoxidase. Tyrosylation of lipoproteins with peroxidase-generated tyrosyl radical generates multiple protein-bound tyrosine oxidation products in addition to dityrosine. The structural characterization of these products would thus serve as an important step in determining the role of myeloperoxidase in lipoprotein oxidation in the artery wall. We now report the identification and characterization of four distinct tyrosyl radical addition products generated by human phagocytes. Activated neutrophils synthesized three major fluorescent products from L-tyrosine; on reverse phase HPLC, each compound coeluted with fluorescent oxidation products formed by myeloperoxidase. We purified the oxidation products to apparent homogeneity by cation and anion exchange chromatographies and identified the compounds as dityrosine (3,3′-dityrosine), trityrosine (3,3′,5′,3″-trityrosine) and pulcherosine (5-[4″-(2-carboxy-2-aminoethyl)phenoxy]3,3′-dityrosine) by high resolution NMR spectroscopy and mass spectrometry. Additionally, we have found that dityrosine is a precursor to trityrosine, but not pulcherosine. In a search for a precursor to pulcherosine, we identified isodityrosine (3-[4′-(2-carboxy-2-aminoethyl)phenoxy]tyrosine), a nonfluorescent product of L-tyrosine oxidation by human phagocytes. Our results represent the first identification of this family of tyrosyl radical addition products in a mammalian system. Moreover, these compounds may serve as markers specific for tyrosyl radical-mediated oxidative damage in atherosclerosis and other inflammatory conditions.

Oxidized low density lipoprotein (LDL)[1] may play a pivotal role in the pathogenesis of atherosclerosis (1–4), but the mechanisms that damage LDL *in vivo* have yet to be identified. A potential pathway involves myeloperoxidase, a heme protein secreted by neutrophils and monocytes (4). Phagocytes employ the myeloperoxidase-H_2O_2 system to generate potent cytotoxins that kill invading pathogens and tumor cells (5–8); under pathological conditions, normal tissue may also be a target for damage. Active myeloperoxidase is a component of human atherosclerotic lesions, where it co-localizes with monocytes and macrophages (9). The pattern of immunostaining for the enzyme in human atherosclerotic lesions (9) is remarkably similar to that for protein-bound lipid oxidation products in rabbit lesions (10), implicating myeloperoxidase as a potential pathway for LDL oxidation *in vivo*.

Hypochlorous acid is the best characterized product of myeloperoxidase (11), which is the only human enzyme known to produce this oxidant under physiological conditions (12). Hypochlorous acid is a potent cytotoxin that oxidatively bleaches heme proteins (13) and chlorinates proteins (14, 15) and unsaturated lipids (16, 17). LDL modified with reagent hypochlorous acid undergoes aggregation and causes macrophages to accumulate cholesteryl ester (18); lipoproteins with similar properties have been isolated from atherosclerotic lesions (19–21). A monoclonal antibody specific for hypochlorous acid-modified proteins recognizes epitopes in human atherosclerotic lesions, as well as LDL-like particles isolated from aortic tissue, strongly suggesting that myeloperoxidase is promoting oxidation in the artery wall (22).

Another substrate for myeloperoxidase is L-tyrosine, which is converted to tyrosyl radical (Scheme I) (23). The major reaction of free tyrosyl radical is dimerization to form the intensely fluorescent amino acid 3,3′-dityrosine (23–26). Tyrosyl radical generated by peroxidase converts protein and lipoprotein tyrosyl residues to dityrosine (27, 28) and initiates LDL lipid peroxidation (29), which may make the lipoprotein atherogenic (1–4).

Tyrosine oxidation products, including dityrosine (30, 31), pulcherosine (32), isodityrosine (33), and trityrosine (30, 32), are a common post-translational modification found in bacteria (34), yeast (35, 36), plants (33), and metazoans (30–33, 37). In

* This work was supported in part by a grant-in-aid from the American Heart Association and by National Institutes of Health Grants RO1 HD29920 and RO1 AG12293. The costs of publication of this article were defrayed in part by the payment of page charges. This article must therefore be hereby marked "*advertisement*" in accordance with 18 U.S.C. Section 1734 solely to indicate this fact.

¶ Supported by a Johnson and Johnson/Merck Research Scholar Award for the American Digestive Health Foundation.

‖ Recipient of a Howard Hughes Postdoctoral Research Fellowship for Physicians.

‡‡ An Established Investigator of the American Heart Association. To whom correspondence should be addressed: Division of Atherosclerosis, Nutrition and Lipid Research, Box 8046, 660 S. Euclid Ave., St. Louis, MO 63110. Tel.: 314-362-6923; Fax: 314-362-3513.

[1] The abbreviations used are: LDL, low density lipoprotein; dityrosine, 3,3′-dityrosine; trityrosine, 3,3′,5′,3″-trityrosine; pulcherosine, 5-[4″-(2-carboxy-2-aminoethyl)phenoxy]-3,3′-dityrosine; isodityrosine, 3-[4′-(2-carboxy-2-aminoethyl) phenoxy]-tyrosine; DTPA, diethylenetriaminepentaacetic acid; HPLC, high pressure liquid chromatography; GC, gas chromatography; MS, mass spectrometry; PMA, phorbol 12-myristate 13-acetate.

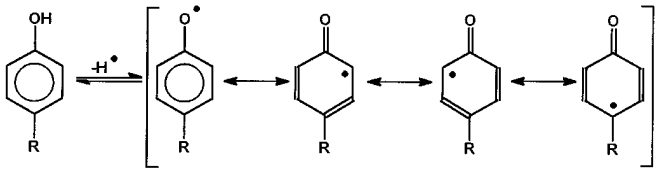

SCHEME I. **Tyrosyl radical generation by hydrogen atom abstraction.**

all cases where the biochemical pathway is known, the mechanism involves direct oxidation of protein tyrosyl residues by a heme protein (30–33, 35, 36). In contrast, myeloperoxidase-catalyzed formation of protein dityrosine cross-links requires free L-tyrosine (28, 29), implying that tyrosyl radical generated by the enzyme is acting as a diffusible radical catalyst. High density lipoprotein exposed to peroxidase-generated tyrosyl radical undergoes tyrosylation and cross-linking of its apolipoproteins by a tyrosine-dependent reaction (27). Examination of acid hydrolysates of high density lipoprotein exposed to L-[^{14}C]tyrosine, H_2O_2, and peroxidase revealed that dityrosine accounted for only 30% of radiolabel incorporated into the protein. Moreover, multiple L-[^{14}C]tyrosine-labeled peaks were present on cellulose phosphate chromatography, suggesting that other products might be formed by tyrosyl radical (27).

We have proposed that dityrosine may serve as a marker for proteins oxidatively damaged by the myeloperoxidase-H_2O_2 system of activated phagocytes (23, 27–29). Recent studies indicate that levels of protein-bound dityrosine are elevated in human atherosclerotic lesions, raising the possibility that tyrosyl radical is a catalyst for LDL oxidation *in vivo*.[2] To search for compounds that might serve as additional markers of phagocyte-mediated protein damage, we examined the ability of myeloperoxidase to catalyze the one electron oxidation of L-tyrosine. We show that human neutrophils employ the myeloperoxidase-H_2O_2 system to generate a family of tyrosyl radical addition products that are acid-stable and strongly fluorescent, making them potentially useful markers for phagocyte-mediated damage *in vivo*.

EXPERIMENTAL PROCEDURES

Materials

Glucose oxidase and crystalline catalase (from beef liver; thymol-free) were purchased from Boehringer Mannheim. L-[$^{13}C_6$]Tyrosine (>99% pure) was from Isotec. All other reagents were from either Sigma or Fisher Scientific unless otherwise indicated.

Methods

Isolation of Myeloperoxidase—Nonidet P-40-treated leukocytes obtained by leukopheresis from a patient with chronic myelogenous leukemia (39) were extracted with cetyltrimethylammonium bromide (40). Myeloperoxidase was then isolated by sequential lectin-affinity chromatography, ammonium sulfate precipitation, and gel filtration chromatography as described previously (23, 40). Myeloperoxidase concentration was determined spectrophotometrically (ϵ_{430} = 170 mM^{-1} cm^{-1}; Ref. 41) and the isolated enzyme had an A_{430}/A_{280} ratio of 0.71.

L-Tyrosine Oxidation by Myeloperoxidase—Reactions were carried out in buffer A (50 mM phosphate, 100 μM DTPA, pH 7.4), which had been passed over a Chelex-100 column (Bio-Rad) to remove metal ions. The reaction mixture contained a final concentration of 2 mM L-tyrosine, 4 nM myeloperoxidase, 1 mg/ml glucose, and 50 ng/ml glucose oxidase. After a 2-h incubatation at 37 °C, the reaction was terminated by addition of catalase (400 nM) and the reaction mixture was stored at −20 °C until analysis.

Isolation of L-Tyrosine Oxidation Products by Ion Exchange Chromatography—Reaction mixture (1 liter) was acidified to pH 3.0 with HCl and subjected to strong cation exchange chromatography (AG-50WX2; Bio-Rad) as a desalting step. The column was eluted with 2 M NH_4OH. The resulting amino acid solution was lyophilized, dissolved in buffer B (10 mM acetic acid, pH 3.0), and then subjected to fast protein liquid chromatography (FPLC) on a Pharmacia Mono S HR 5/5 column equilibrated with buffer B. Amino acids were eluted from the cation exchange column with a 60-ml linear gradient of 0–0.25 M NaCl in buffer B at a flow rate of 1 ml/min. Collected peaks were desalted as above, dissolved in buffer C (10 mM Tris base, pH 9.0), subjected to FPLC on a Pharmacia Mono Q HR 5/5 anion exchange column equilibrated with buffer C, and eluted with a 60-ml linear gradient of 0–0.25 M NaCl in buffer C at 1 ml/min. Each amino acid was then desalted and again subjected to cation exchange chromatography as described above.

L-Tyrosine Oxidation by Activated Human Neutrophils—Neutrophils were prepared from human blood anticoagulated with EDTA (5.4 mM) using Polymorph-Prep (Nycomed, Sunnyvale, CA) as described previously (23). Freshly harvested cells were resuspended in medium A (Ca^{2+}-, Mg^{2+}-, and phenol red-free Hank's balanced salt solution, pH 7.4; Life Technologies, Inc.) and used immediately for experiments. Reactions were carried out at 37 °C in medium A supplemented with 1 mM L-tyrosine, 0.1 mM DTPA, and 1 mg/ml D-glucose. Neutrophils (5×10^5 cells/ml) were activated by the addition of of 200 nM phorbol 12-myristate 13-acetate (PMA; dissolved in dimethyl sulfoxide) and were maintained in suspension by periodic inversion. Reactions were stopped by the addition of 400 nM catalase, the cells were pelleted by centrifugation, and the supernatant was stored at −20 °C until analysis. Superoxide ($O_2^{\cdot-}$) production by neutrophils was measured as the superoxide dismutase-inhibitable reduction of ferricytochrome *c* (23).

Reverse Phase HPLC Analysis of Fluorescent Neutrophil and Myeloperoxidase Reaction Products—Oxidation reactions were filtered (Acrodisc LC PVDF, 0.2 μm; Gelman Sciences) and analyzed on a Beckman Ultrasphere ODS column (250 × 4.6 mm, 5-μm diameter particles). Products were eluted isocratically at 2 ml/min with a mobile phase of 0.1 M Na_2HPO_4, 0.1 mM EDTA adjusted to pH 5.9 with acetic acid. L-tyrosine was detected by absorbance (280 nm) using a Beckman model 163 variable wavelength detector. Fluorescent compounds were detected with a Waters model 470 scanning fluorescence detector (λ_{ex} 296 nm, λ_{em} 414 nm).

NMR Spectroscopy—One- and two-dimensional NMR spectra were acquired at 25 °C using a Varian Unity 500 spectrometer (499.843 MHz for ^{1}H) interfaced to a Sun SPARC-2 workstation and equipped with a Nalorac triple-resonance indirect-detection probe. Prior to analysis, FPLC-purified products were dissolved in D_2O (Cambridge Isotope Laboratories). Proton and carbon-13 chemical shifts were referenced to external sodium 3-(trimethylsilyl)propionate-2,2,3,3-d_4 in D_2O. For two-dimensional experiments, data were acquired in the hypercomplex mode (42).

Gas Chromatography-Mass Spectrometry (GC-MS)—FPLC-purified and desalted oxidation products were evaporated under N_2 and esterified by incubation with 200 μl of HBr (3.5 M) in *n*-propanol (Cambridge Isotope Laboratories) at 100 °C for 30 min. Pentafluoropropyl derivatives were then prepared by incubation of dried propylated amino acids with 50 μl of ethyl acetate/pentafluoropropionic acid anhydride (4:1, v/v) at 60 °C for 30 min. Derivatized amino acids were stored in reagent solution until analysis.

GC and direct probe MS analyses were obtained with a HP-5988A mass spectrometer equipped with a Technivent Vector 1 Data System. Capillary GC was performed using a DB-1 column (8 m, 0.33 mm inner diameter, 1-μm film thickness; J & W Scientific) in the splitless injection mode. The initial column temperature of 70 °C was increased to 150 °C at 60 °C/min, and then to 250 °C at 10 °C/min. The injector, transfer line, and ion source temperature were set at 220 °C, 250 °C, and 150 °C, respectively. Mass spectra were obtained in the negative-ion chemical ionization mode using methane as the reagent gas.

RESULTS

Myeloperoxidase Generates a Family of Tyrosyl Radical Addition Products—Three major fluorescent peaks, termed compounds I, II, and III, were identified by Mono S chromatography when L-tyrosine was oxidized by the myeloperoxidase-H_2O_2 system (Fig. 1). Production of all three oxidation products required active myeloperoxidase and the H_2O_2 generating system and was inhibited by catalase (a scavenger of H_2O_2), azide (a heme poison), and ascorbate (which reacts with both H_2O_2 and tyrosyl radical). Compounds I, II, and III eluted from a Mono S cation exchange column at 60 mM, 115 mM, and 105 mM NaCl, respectively; compound I coeluted with authentic dityrosine. Each of the products exhibited dityrosine-like fluores-

[2] J. E. Rasmussen and J. W. Heinecke, unpublished observation.

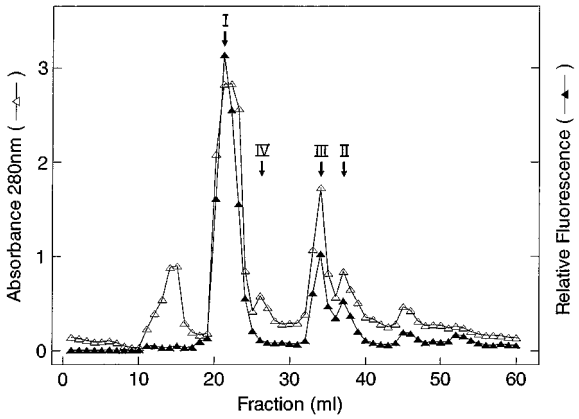

FIG. 1. **Cation exchange FPLC analysis of the L-tyrosine oxidation products generated by myeloperoxidase.** L-Tyrosine (2 mM) in buffer A (1 liter) was incubated with myeloperoxidase (4 nM) and an H_2O_2 generating system (100 ng/ml glucose oxidase and 0.1 mg/ml D-glucose). After a 2-h incubation at 37 °C, the reaction was terminated by the addition of catalase (400 nM). The reaction mixture was desalted and subjected to FPLC on a Mono S HR 5/5 column as described under "Methods." The peaks of material labeled *I*, *II*, *III*, and *IV* were purified to apparent homogeneity by sequential chromatography on anion exchange (Mono Q HR5/5) and cation exchange (Mono S HR5/5) columns, and subsequently identified as dityrosine, pulcherosine, trityrosine, and isodityrosine, respectively, in the structural studies described under "Results."

cence (λ_{ex} 315 nm and λ_{em} 410 nm, respectively, pH 9.0) and tyrosine-like absorbance (λ_{max}, ~280 nm, pH 3.0). Each fluorescent peak was collected, desalted and subjected to chromatography on a Mono Q column as described under "Methods." Compounds I, II, and III eluted from the anion exchange column at 135, 145, and 180 mM NaCl, respectively. The purified oxidation products employed for the structural studies described below were apparently homogeneous as assessed by repeat Mono S chromatography as well as by reverse phase HPLC; each compound eluted as a single, symmetrical peak as monitored by both fluorescence and absorbance.

Structural Characterization of the Fluorescent L-Tyrosine Oxidation Products Generated by Myeloperoxidase—^{1}H NMR resonances from the aromatic region (6.8–7.4 ppm) of compounds I, II and III and their structural assignments are shown in Fig. 2. This region of compound I (Fig. 2*A*) was very similar to that previously reported for 3,3′-dityrosine isolated from yeast spore coats (32) and contained 6 protons with chemical shifts of: 6.99 (H_a), 7.14 (H_b), and 7.23 ppm (H_c). Compound III exhibited 8 protons in the aromatic region (Fig. 2*B*): 6.98 (H_a), 7.24 (H_b), 7.33 (H_d), and 7.36 ppm (H_c) and is consistent with the structure of trityrosine. The spectrum of compound II (Fig. 2*C*) is consonant with the structure of pulcherosine and demonstrated nine aromatic protons: 6.98 (H_a), 7.00 (H_e), 7.02 (H_f), 7.13 (H_d), 7.23 (H_b), 7.29 (H_g), and 7.31 ppm (H_c). To confirm the assignments of the protons in compound II, we used total correlation spectroscopy to examine the connectivities of the protons (Fig. 3). Proton-proton correlations between the single proton peaks at 6.96 (H_a) and 7.23 ppm (H_b), and the two proton peaks at 7.02 (H_f) and 7.28 ppm (H_g), indicate that the protons are adjacent to one another on the aromatic ring. Correlation between peaks at 7.01 (H_e) and 7.12 ppm (H_d) and the peaks at 7.23 (H_b) and 7.32 ppm (H_c) are indicative of four bond, long-range interactions. These data are consistent with the structure of pulcherosine.

Mass spectrometry was used to confirm the proposed structures of compounds I, II and IlI. The *n*-propyl ester, pentafluoropropyl derivative of each compound was prepared, and the dityrosine and pulcherosine derivatives subjected to GC-MS in the negative-ion chemical ionization mode. Because it was relatively non-volatile, derivatized trityrosine was analyzed using direct probe MS. Dityrosine exhibited a low abundance ion peak at mass-to-charge (*m*/*z*) 1028, the calculated molecular ion (M^-) for the derivative. Prominent ions were observed at *m*/*z* 1008 $(M - HF)^-$ and 880 $(M - CF_3\,CF_2CHO)^-$. The mass spectrum of derivatized pulcherosine demonstrated a low abundance ion at *m*/*z* 1395 (M^-) and major fragment ions at *m*/*z* 1375 $(M - HF)^-$ and 1247 $(M - CF_3\,CF_2CHO)^-$. The trityrosine derivative exhibited a low abundance ion at m/z

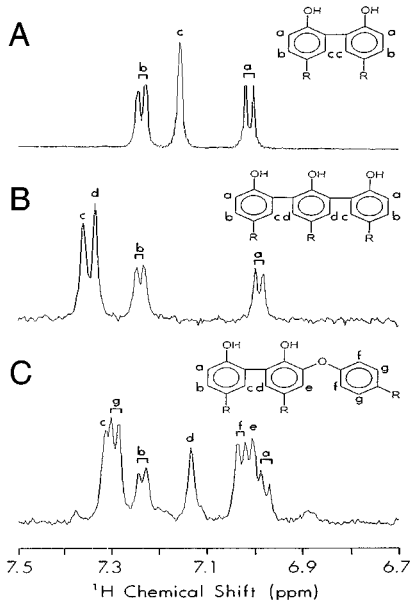

FIG. 2. **Aromatic region of 500-MHz ^{1}H NMR spectra of dityrosine, trityrosine, and pulcherosine.** *Insets* show the structures of dityrosine (*A*), trityrosine (*B*), and pulcherosine (*C*) with the assignments of aromatic protons; spin-spin coupling interactions are indicated where known.The spectra were processed with pseudo-echo apodization with a line broadening of −5 Hz and a Gaussian time constant of 0.05 s. Number of transients, 64; number of time-domain points, 8192; spectral width, 6000 Hz.

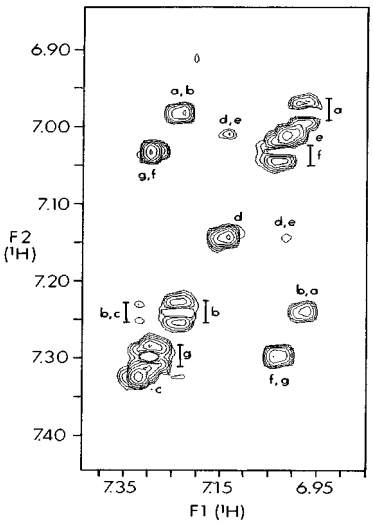

FIG. 3. **Aromatic region of the two-dimensional total correlation spectrum of pulcherosine.** The sample used for this spectrum was identical to that in Fig. 2*C*. The cross-peak labels separated by *commas* represent through-bond correlations between protons resulting from scalar couplings. The spectrum was processed with pseudo-echo weighting in F2 (line broadening, −6 Hz; Gaussian time constant, 0.06 s) and Gaussian weighting in F1 (time constant, 0.047 s). The pulse sequence was that of Bax and Davis (53). Mixing time, 20 ms; number of transients, 24; time domain points in *t2*, 4096; spectral width (F2 and F1), 6000 Hz; number of *t1* increments, 512 zero filled to 1024.

TABLE I
Spectroscopic properties of dityrosine, trityrosine, and pulcherosine
UV spectra were obtained in 0.1 M HCl or 0.1 M NH_4OH. Fluorescence excitation and emission spectra were obtained in 0.1 M HCl or 0.1 M NaOH with excitation and emission slits of 5 and 10 nm, respectively.

	Absorbance		Fluorescence (λ_{max})	
	ϵ_{max}	λ_{max}	Excitation	Emission
	$M^{-1}cm^{-1}$	*nm*	*nm*	*nm*
Dityrosine				
Acid	5,400	284	284	409
Base	8,600	316	317	407
Trityrosine				
Acid	11,000	286	286	409
Base	11,500	322	319	416
Pulcherosine				
Acid	7,700	282	283	416
Base	9,500	315	320	414

1541(M^-), as well as major ions expected from loss of HF and CF_3 CF_2CHO at *m/z* 1521 and 1393, respectively. The mass spectra of compounds I, II, and III are thus in excellent agreement with the structures determined using multinuclear NMR spectroscopy.

Ultraviolet Absorption and Fluorescence Spectra with Molar Extinction Coefficient Determinations of the Major Tyrosyl Radical Addition Products—Radiolabeled dityrosine, pulcherosine, and trityrosine were isolated by FPLC from an L-[^{14}C]tyrosine solution of known specific activity oxidized with myeloperoxidase, and their concentrations determined by scintillation spectrometry. The extinction coefficients, ultraviolet absorption spectra, and fluorescence excitation/emission spectra of the compounds were then determined at acid and alkaline pH. These data, which are in good agreement with previously reported results for tyrosine oxidation products isolated from sea urchins, insects, and yeast (24, 25, 32, 36), are summarized in Table I.

Isolation and Identification of Isodityrosine, a Non-fluorescent L-Tyrosine Radical Addition Product Generated by Myeloperoxidase—Initial fractionation of the myeloperoxidase-L-tyrosine-H_2O_2 reaction mixture revealed a small shoulder of material, which eluted just after dityrosine on cation exchange chromatography (Fig. 1, *peak IV*). This material exhibited tyrosine-like absorbance but not dityrosine-like fluorescence. To investigate the structure of this compound, L-[$^{13}C_6$]tyrosine in buffer A was exposed to the myeloperoxidase-H_2O_2 system, and the product was isolated by sequential cation, anion, and cation exchange FPLC as described above for compounds I–III. The isolated compound, which eluted as a single, symmetrical peak on reverse phase HPLC analysis, was subjected to heteronuclear single quantum coherence NMR spectroscopy (Fig. 4). The compound exhibited 5 distinct proton-carbon bonds in the aromatic region. These represented 7 protons in the aromatic region with the following shifts: 6.75–123 (H_a), 6.80–125 (H_c), 6.90–129.5 (H_b), 6.90–119 (H_d), and 7.20–133 (H_e). This spectrum is consistent with the structure of isodityrosine. The negative-ion chemical ionization mass spectrum of the *n*-propyl ester, pentafluoropropyl derivative revealed an ion at *m/z* 894 (M^-), with fragment ions at 874 $(M - HF)^-$ and 746 $(M - CF_3$ $CF_2CHO)^-$, which confirmed the identity of the non-fluorescent compound as [$^{13}C_{12}$]isodityrosine.

Isodityrosine might be an intermediate in the synthesis of pulcherosine by myeloperoxidase. To test this hypothesis, we supplemented the complete myeloperoxidase-H_2O_2 system with 1 mM L-tyrosine and 0.02 mM isodityrosine, and then monitored the formation of pulcherosine. The yield of pulcherosine increased 2-fold in the presence of isodityrosine whereas the formation of trityrosine was unaffected. In contrast, the presence of dityrosine (0.02 mM) caused a 3-fold increase in the yield of trityrosine, but did not affect the yield of pulcherosine. These results strongly suggest that isodityrosine and dityrosine are intermediates in the formation of pulcherosine and trityrosine, respectively.

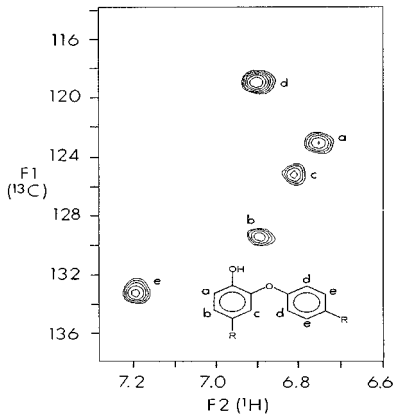

FIG. 4. **Aromatic region of the two-dimensional ^{1}H-^{13}C heteronuclear single quantum correlation of [*ring*-$^{13}C_{12}$]-isodityrosine.** *Inset* shows the assignment of hydrogen atoms. The pulse sequence was that of Bax *et al.* (38), and carbon decoupling during acquisition was achieved using Waltz-16. Gaussian apodization was employed in both dimensions with time constants of 0.031 and 0.015 s in F2 and F1, respectively. Number of transients, 32; time domain points in *t2*, 2048; spectral width (F2), 6000 Hz; number of increments, 64; spectral width (F1), 5028 Hz.

Neutrophils Employ the Myeloperoxidase-H_2O_2 System to Convert L-Tyrosine to Dityrosine, Trityrosine, Pulcherosine, and Isodityrosine—To explore the possibility that the family of tyrosyl radical addition products generated by myeloperoxidase are indices of phagocyte activation, we used reverse phase HPLC with fluorescence monitoring to quantify the synthesis of each compound by phorbol ester-stimulated human neutrophils. Cells were incubated at 37 °C in a physiological salt solution supplemented with 1 mM L-tyrosine and 0.1 mM DTPA. Three peaks with dityrosine-like fluorescence were observed that co-migrated with authentic dityrosine, trityrosine, and pulcherosine generated by the myeloperoxidase-H_2O_2 system (Fig. 5). The identity of the neutrophil-generated fluorescent compounds was confirmed by demonstrating co-migration with each myeloperoxidase-generated oxidation product on two independent reverse phase HPLC systems (43) and on anion and cation exchange FPLC. The non-fluorescent product, isodityrosine, was readily identified by GC-MS analysis, but was below the UV detection limit on HPLC.

Production of dityrosine, trityrosine, and pulcherosine required phagocytes, L-tyrosine, and activation of the cells by phorbol ester (Table II). L-Tyrosine oxidation by the cells was independent of iron or copper because the buffer contained DTPA, a potent inhibitor of metal-catalyzed reactions (44). As with the reaction catalyzed by purified myeloperoxidase, the neutrophil reaction was inhibited by catalase, by the heme poisons azide and cyanide, and by ascorbate (Table II). Collectively, these results suggest that the family of tyrosyl radical addition products generated by myeloperoxidase constitutes molecular markers of phagocyte activation.

Dityrosine Promotes the Synthesis of Trityrosine by Neutrophils—Studies with isolated myeloperoxidase suggested that isodityrosine and dityrosine were precursors for pulcherosine and trityrosine, respectively. To test the hypothesis that dityrosine was similarly employed by the myeloperoxidase system of activated human neutrophils to generate trityrosine, we supplemented the medium of neutrophils with dityrosine (0.01 mM) and L-tyrosine (1 mM) and then monitored the kinetics of trityrosine and pulcherosine synthesis. The presence of dity-

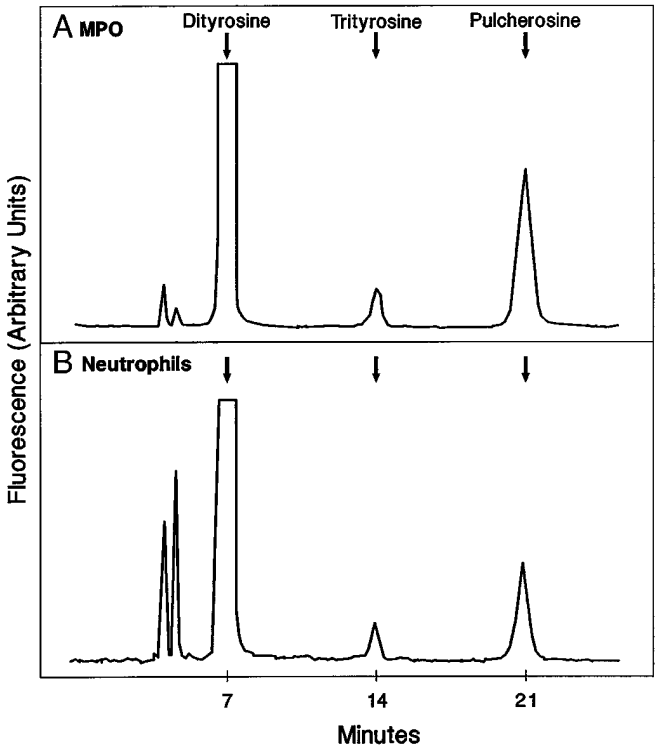

FIG. 5. **Reverse phase HPLC analysis of fluorescent tyrosine oxidation products generated by myeloperoxidase (*A*) and activated human neutrophils (*B*).** L-Tyrosine was oxidized either with the myeloperoxidase-H_2O_2 system as described in the legend to Fig. 1 or with activated human neutrophils as described in the legend to Fig. 6. After a 2-h incubation at 37 °C, the reactions were terminated by addition of catalase (400 nM) and subjected to analysis by reverse phase HPLC as described under "Methods." Tyrosine oxidation products were detected by monitoring fluorescence (λ_{ex} 296 nm, λ_{em} 414 nm).

TABLE II
Requirements for dityrosine, trityrosine, and pulcherosine synthesis by neutrophils

Oxidation of L-tyrosine by neutrophils (5×10^5 cells/ml) was carried out in medium A supplemented with 0.1 mM DTPA, 1 mg/ml D-glucose, and 1 mM L-tyrosine. Neutrophils were activated by the addition of 200 nM PMA. After a 2-h incubation at 37 °C, the reaction was stopped by the addition of 400 nM catalase. Samples were analyzed by reverse phase HPLC as described under "Methods." The limit of detection for each compound was less than 1 pmol. Values are expressed as picomoles per 5×10^5 cells and are the mean of duplicate determinations. Similar results were found in two independent experiments.

	Dityrosine	Trityrosine	Pulcherosine
		pmol	
Complete system	691	86	20
Complete system plus:			
Superoxide dismutase (150 nM)	1531	1024	256
Catalase (400 nM)	26	<1	<1
CN^- (5 mM)	88	<1	<1
N_3^- (0.6 mM)	112	<1	<1
Ascorbate (0.5 mM)	20	<1	<1
Complete system minus:			
L-Tyrosine	<1	<1	<1
Cells	38	<1	<1
Phorbol myristate acetate	55	<1	<1

rosine led to a decrease in the lag phase for trityrosine synthesis (Fig. 6, *upper panel*). Moreover, there was a dramatic 8-fold increase in the yield of trityrosine. These results strongly suggest that dityrosine is a precursor in the generation of trityrosine. In contrast to trityrosine, the kinetics and yield of pulcherosine (Fig. 6, *lower panel*) were unaffected by the presence of dityrosine, suggesting that pulcherosine generation involves another intermediate. These results suggest that tyrosyl radical reacts by two different pathways to generate trityrosine and pulcherosine.

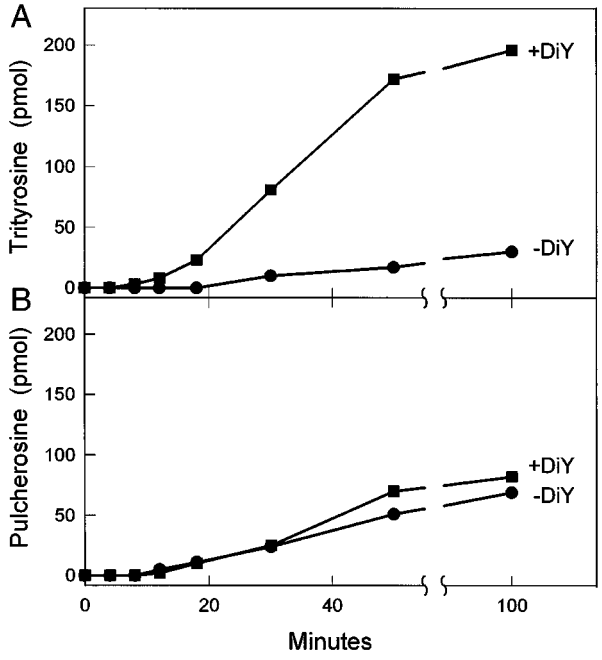

FIG. 6. **Progress curve for trityrosine (*A*) and pulcherosine synthesis (*B*) by human neutrophils in the presence and absence of dityrosine.** Neutrophils (5×10^5 cells/ml) were incubated at 37 °C in medium A supplemented with 1 mM L-tyrosine, 0.1 mM DTPA and 1 mg/ml D-glucose. Where indicated, dityrosine (*DiY*; 10 μM) was included. After stimulation of the cells with 200 nM PMA, aliquots of medium were removed at the indicated times and trityrosine and pulcherosine production quantified by reverse phase HPLC as described under "Methods." Values are expressed as picomoles per 5×10^5 cells and represent the mean of duplicate determinations.

Superoxide Dismutase Stimulates L-Tyrosine Oxidation by Activated Neutrophils—The initial product of the neutrophil oxidase is $O_2^{\cdot-}$, the one-electron reduced form of molecular oxygen (45). $O_2^{\cdot-}$ scavenges tyrosyl radical by acting as an electron donor (46, 47). This reaction is blocked by superoxide dismutase, which catalyzes the dismutation of $O_2^{\cdot-}$ to H_2O_2 (46, 47). To explore the role of $O_2^{\cdot-}$ in L-tyrosine oxidation, the kinetics of dityrosine, trityrosine, and pulcherosine generation by activated neutrophils in the presence and absence of superoxide dismutase were monitored. Neutrophil activation resulted in $O_2^{\cdot-}$ production after a lag phase of ~2 min (data not shown). The progress curve of dityrosine production was similarly nonlinear but with a longer lag phase of ~6 min (Fig. 7, *top panel*). In contrast, the lag phases for $O_2^{\cdot-}$ generation and dityrosine synthesis were virtually identical when superoxide dismutase was included. Catalase inhibited the production of dityrosine, trityrosine, and pulchosine by neutrophils (Fig. 7), confirming that H_2O_2 is necessary for their synthesis.

The progress curves for both pulcherosine and trityrosine production by activated neutrophils exhibited lag phases that were greater than that observed for dityrosine (Fig. 7). As with dityrosine, superoxide dismutase significantly shortened the lag phases for trityrosine and pulcherosine production (Fig. 7, *middle* and *bottom panels*). Superoxide dismutase led to a 1.5-fold increase in dityrosine and 8- and 4-fold increases in trityrosine and pulcherosine, respectively. Superoxide dismutase may have stimulated the yield of L-tyrosine oxidation products by blocking the scavenging of tyrosyl radical by $O_2^{\cdot-}$ (46, 47), by preventing the formation of an inactive form of myeloperoxidase (48), or by increasing the yield of H_2O_2 from $O_2^{\cdot-}$ (45).

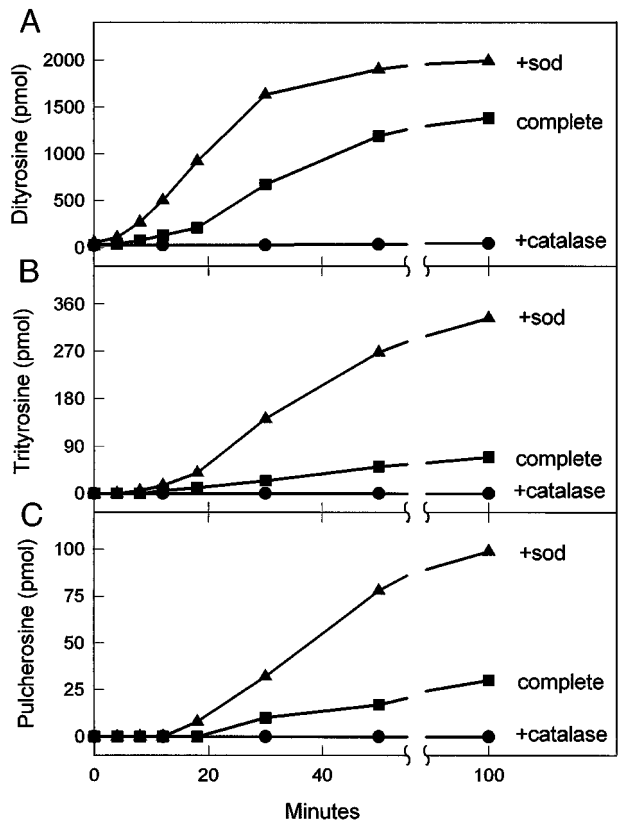

FIG. 7. **Progress curves for the synthesis of dityrosine (*A*), trityrosine (*B*), and pulcherosine (*C*) by activated human neutrophils.** Neutrophils (5×10^5 cells/ml) were incubated at 37 °C in medium A supplemented with 1 mM L-tyrosine, 0.1 mM DTPA, and 1 mg/ml D-glucose. Where indicated, superoxide dismutase (*sod*; 150 nM) or catalase (400 nM) were included in the medium. After stimulation of the cells with 200 nM PMA, aliquots of the medium were removed at the indicated times and subjected to analysis by reverse phase HPLC as described under "Methods." Values are expressed as picomoles per 5×10^5 cells and represent the mean of duplicate determinations.

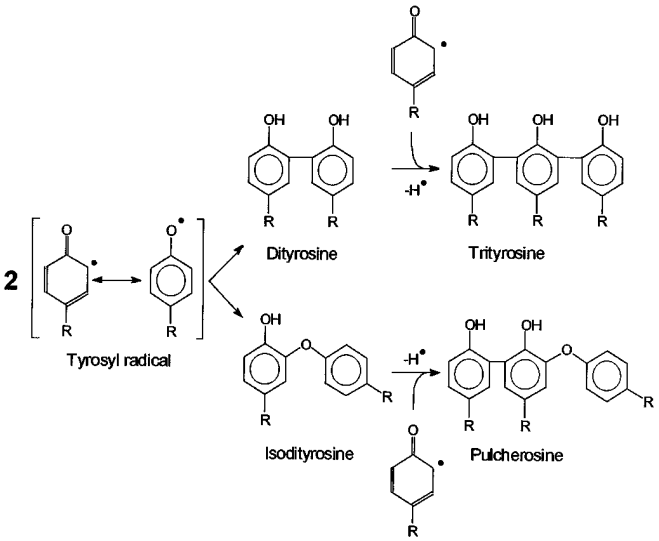

SCHEME II. **Proposed reaction pathways for the generation of tyrosyl radical addition products by myeloperoxidase.** The proposed pathway for trityrosine production involves conversion of dityrosine to dityrosyl radical, which cross-links with a free tyrosyl radical to form trityrosine. Dityrosine might be oxidized directly by myeloperoxidase or indirectly by tyrosyl radical. Indeed, recent kinetic studies demonstrate that dityrosine is an excellent substrate for oxidation by myeloperoxidase (51). In light of the evidence that isodityrosine increases the formation of pulcherosine by myeloperoxidase, it is likely that this compound is similarly an intermediate in pulcherosine formation. Isodityrosine would then be oxidized to a radical which cross-links with tyrosyl radical to generate pulcherosine.

DISCUSSION

Several lines of evidence indicate that human neutrophils employ the myeloperoxidase-H_2O_2 system to convert L-tyrosine to tyrosyl radical, which then undergoes radical addition reactions to form dityrosine, isodityrosine, trityrosine, and pulcherosine. First, purified myeloperoxidase converted L-tyrosine to three fluorescent products and one non-fluorescent product by a reaction that required H_2O_2 and was sensitive to inhibition by heme poisons. The products of this reaction were identified as dityrosine, isodityrosine, trityrosine, and pulcherosine by NMR and mass spectroscopy. Second, activation of human neutrophils with phorbol ester led to the formation of the identical family of tyrosyl radical addition products. As with myeloperoxidase, synthesis of the compounds required H_2O_2 and was inhibited by heme poisons. Finally, the formation of dityrosine, trityrosine and pulcherosine by activated neutrophils was inhibited by ascorbic acid and stimulated by superoxide dismutase. Both ascorbate and $O_2^{\cdot-}$, the initial product of the neutrophil oxidase (45), are known to repair tyrosyl radical, and the reaction of $O_2^{\cdot-}$ with tyrosyl radical is blocked by superoxide dismutase (46, 47). These results represent the first identification of this family of tyrosyl radical addition products in a mammalian system and suggest their potential as specific markers for phagocyte-mediated oxidative damage.

The one-electron oxidation of L-tyrosine by myeloperoxidase bears striking parallels with the chemistry of phenoxyl radical (49, 50). In both systems, the spectrum of products is readily explained by radical-radical coupling at the predominant sites of electron density on the oxygen and aromatic carbons (Scheme I). Substituents in the *para* position of phenoxyl radical block both *o,p′* and *p,p′* dimerization (49, 50). L-Tyrosine oxidation by myeloperoxidase generates the products expected from *para*-substituted phenoxyl radical, including compounds with carbon-carbon cross-links (dityrosine, trityrosine, pulcherosine) and carbon-oxygen cross-links (pulcherosine and isodityrosine), strongly implicating tyrosyl radical in the reaction pathway.

Three observations suggest that dityrosine itself might be oxidized by activated neutrophils to dityrosyl radical, which then reacts with tyrosyl radical to form trityrosine. First, the lag phase for the conversion of L-tyrosine to trityrosine by the cells was significantly greater than that observed for dityrosine, suggesting that trityrosine production was dependent upon dityrosine formation. Second, the lag phases for the synthesis of both dityrosine and trityrosine were shortened by superoxide dismutase; this enzyme scavenges $O_2^{\cdot-}$, which is known to repair tyrosyl radical (46, 47). Third, when a low concentration of dityrosine was included together with L-tyrosine in the medium of the cells, the lag phase for trityrosine synthesis was shortened and the yield of the compound was increased 8-fold. In contrast, dityrosine had little effect on either the progress curve or the yield of pulcherosine. Scheme II is consistent with these results and the chemistry of phenoxyl radical (49, 50).

Oxidation of LDL may represent an important step in conferring atherogenic potential to the modified lipoprotein. However, the biochemical pathways that mediate LDL oxidation *in vivo* have yet to be identified (1–4). Previously, we have shown that active myeloperoxidase is expressed in human atherosclerotic lesions (9) and that myeloperoxidase-derived tyrosyl radical initiates LDL lipid peroxidation (29). LDL isolated from vascular tissue exhibits evidence of lipid peroxidation (19–21) and is aggregated (21), suggesting that tyrosyl radical may account in part for intermolecular cross-linking of artery wall

lipoproteins. L-Tyrosine oxidation may also play a role in stimulating the cellular uptake of lipoproteins because cross-linking causes LDL to aggregate and stimulates its uptake by macrophages (18, 21, 22, 52).

Tyrosyl radical generated by activated phagocytes causes protein tyrosylation (28), and human atherosclerotic lesions contain elevated levels of protein-bound dityrosine,[2] implicating peroxidative pathways as one mechanism for oxidative damage of the vascular wall. The L-tyrosine oxidation products we have described are stable to acid hydrolysis, intensely fluorescent, and readily detected by mass spectrometry, making them attractive candidates for monitoring protein oxidative damage. Moreover, dityrosine accounts for only a third of the L-tyrosine covalently incorporated into the apolipoproteins of high density lipoprotein exposed to tyrosyl radical (27), supporting our hypothesis that myeloperoxidase-damaged proteins may contain multiple significant L-tyrosine oxidation products. The detection of trityrosine, isodityrosine, and pulcherosine in proteins tyrosylated by myeloperoxidase *in vitro*, and the demonstration that a similar pattern of protein-bound oxidation products exists in human vascular lesions, would strongly support our hypothesis that tyrosyl radical generated by myeloperoxidase plays a critical role in oxidative damage during atherosclerosis and inflammation.

Acknowledgments—Gas chromatography-mass spectrometry experiments were performed at the Washington University School of Medicine Mass Spectrometry Resource (supported by National Institute of Health Grant RR00954).

REFERENCES

1. Witztum, J. L., and Steinberg, D. (1991) *J. Clin. Invest.* **88,** 1785–1792
2. Esterbauer, H., Wagner, G., and Puhl, H. (1993) *Br. Med. Bull.* **49,** 566–576
3. Lusis, A. J., and Navab, M. (1993) *Biochem. Pharm.* **46,** 2119–2126
4. Berliner, J. A., and Heinecke, J. W. (1996) *Free Radical Biol. Med.* **20,** 707–727
5. Babior, B. M. (1978) *N. Engl. J. Med.* **298,** 659–663
6. Klebanoff, S. J. (1980) *Ann. Intern. Med.* **93,** 480–489
7. Weiss, S. J. (1989) *N. Engl. J. Med.* **320,** 365–376
8. Hurst, J. K., and Barrette, W. C., Jr. (1989) *CRC Crit. Rev. Biochem. Mol. Biol.* **24,** 271–328
9. Daugherty, A., Dunn, J. L., Rateri, D. L., and Heinecke, J. W. (1994) *J. Clin. Invest.* **94,** 437–444
10. Rosenfeld, M. E., Palinski, W., Yla-Herttuala, S., Butler, S., and Witztum, J. L. (1990) *Arteriosclerosis* **10,** 336–349
11. Harrison, J. E., and Schultz, J. (1976) *J. Biol. Chem.* **251,** 1371–1374
12. Weiss, S. J., Test, S. T., Eckmann, C. M., Ross, D., and Regiani, S. (1986) *Science* **234,** 200–203
13. Albrich, J. M., McCarthy, C. A., and Hurst, J. K. (1981) *Proc. Natl. Acad. Sci. U. S. A.* **78,** 210–214
14. Thomas, E. L., Jefferson, M. M., and Grisham, M. B. (1982) *Biochemistry* **21,** 6299–6308
15. Vissers, M. C. M., and Winterbourn, C. C. (1991) *Arch. Biochem. Biophys.* **285,** 53–59
16. Winterbourn, C. C., Van den Berg, J. J. M., Roitman, E., and Kuypers, F. A. (1992) *Arch. Biochem. Biophys.* **296,** 547–555
17. Heinecke, J. W., Li, W., Mueller, D. M., Bohrer, A., and Turk, J. (1994) *Biochemistry* **33,** 10127–10136
18. Hazell, L. J., and Stocker, R. (1993) *Biochem. J.* **290,** 165–172
19. Daugherty, A., Zweifel, B. S., Sobel, B. E., and Schonfeld, G. (1988) *Arteriosclerosis* **8,** 768–777
20. Yla-Herttuala, S., Palinski, W., Rosenfeld, M. E., Parathasarathy, S., Carew, T. E., Butler, S., Witztum, J. L., and Steinberg, D. (l989) *J. Clin. Invest.* **84,** 1086–1095
21. Steinbrecher, U. P., and Lougheed, M. (1992) *Arterioscler. Thromb.* **12,** 608–625
22. Hazell, L. J., Arnold, L., Flowers, D., Waeg, G., Malle, E., and Stocker, R. (1996) *J. Clin. Invest.* **97,** 1535–1544
23. Heinecke, J. W., Li, W., Daehnke, H. L., III, and Goldstein, J. A. (1993) *J. Biol. Chem.* **268,** 4069–4077
24. Gross, A. J., and Sizer, I. W. (1959) *J. Biol. Chem.* **234,** 1611–1614
25. Anderson, S. O. (1966) *Acta Physiol. Scand.* **66,** 1–81
26. Amado, R., Aeschbach, R., and Neukom, H. (1984) *Methods Enzymol.* **107,** 377–388
27. Francis, G. A., Mendez, A. J., Bierman, E. L., Heinecke, J. W. (1993) *Proc. Natl. Acad. Sci. U. S. A.* **90,** 6631–6635
28. Heinecke, J. W., Li, W., Francis, G. A., and Goldstein, J. A. (1993) *J. Clin. Invest.* **91,** 2866–2872
29. Savenkova, M. I., Mueller, D. M., and Heinecke, J. W. (1994) *J. Biol. Chem.* **269,** 20394–20400
30. Foerder, C. A., and Shapiro, B. M. (1977) *Proc. Natl. Acad. Sci. U. S. A.* **74,** 4214–4218
31. Deits, T., Forrance, M., Kay, E. S., Medill, L., Turner, E. E., Weidman, P. J., and Shapiro, B. M. (1984) *J. Biol. Chem.* **259,** 13525–13533
32. Nomura, K., Suzuki, N., and Matsumoto, S. (1990) *Biochemistry* **29,** 4525–4534
33. Fry, S. C. (1982) *Biochem. J.* **204,** 449–455
34. Pandey, N. K., and Aronson, A. I. (1979) *J. Bacteriol.* **137,** 1208–1218
35. Briza, P., Winkler, G., Kalchhauser, H., and Breitenbach, M. (1986) *J. Biol. Chem.* **261,** 4288–4294
36. Briza, P., Breitenbach, M., Ellinger, A., and Segall, J. (1990) *Genes Dev.* **4,** 1775–1789
37. Raven, D. J., Earland, C., and Little, M. (1971) *Biochim. Biophys. Acta* **251,** 96–99
38. Bax, A., Ikura, M., Kay, L. E., Torchia, D. A., and Tschudin, R. (1990) *J. Magn. Reson.* **86,** 304–318
39. Hickstein, D. D., Ozols, J., Williams, S. A., Baenziger, J. U., Locksley, R. M., and Roth, G. J. (1987) *J. Biol. Chem.* **262,** 5576–5580
40. Rakita, R. M., Michel, B. R., and Rosen, H. (1990) *Biochemistry* **29,** 1075–1080
41. Morita, Y., Iwamoto, H., Aibara, S., Kobayashi, T., and Hasegawa, E. (1986) *J. Biochem.* (*Tokyo*) **99,** 761–770
42. States, D. J., Haberkon, R. A., and Reuben, D. J. (1983) *J. Magn. Reson.* **48,** 286–292
43. Hazen, S. L., Hsu, F. F., and Heinecke, J. W. (1996) *J. Biol. Chem.* **271,** 1861–1867
44. Heinecke, J. W., Baker, L., Rosen, H., and Chait, A. (1986) *J. Clin. Invest.* **77,** 757–761
45. Babior, B. M., Kipnes, R. S., and Curnutte, J. T. (1973) *J. Clin. Invest.* **52,** 741–744
46. Prutz, W. A., Kira, A., and Land, E. J. (1983) *Int. J. Radiat. Biol.* **44,** 183–196
47. Hunter, E. P. L., Desrosiers, M. F., and Simic, M. G. (1989) *Free Radical Biol. Med.* **6,** 581–585
48. Kettle, A. J., Sangster, D. F., Gebicki, J. M., and Winterbourn, C. C. (1988) *Biochim. Biophys. Acta* **956,** 58–62
49. Scott, A. I. (1965) *Q. Rev.* (*London*) **19,** 1–35
50. Musso, H. (1963) *Angew. Chem. Int. Edit.* **2,** 723–735
51. Marquez, L. A., and Dunford, H. B. (1995) *J. Biol. Chem.* **270,** 30434–30440
52. Hoff, H. F., Whitaker, T. E., and O'Neil, J. (1992) *J. Biol. Chem.* **267,** 602–609
53. Bax, A., and Davis, D. G. (1985) *J. Magn. Reson.* **65,** 355–360

Human Phagocytes Employ the Myeloperoxidase-Hydrogen Peroxide System to Synthesize Dityrosine, Trityrosine, Pulcherosine, and Isodityrosine by a Tyrosyl Radical-dependent Pathway

Jason S. Jacob, David P. Cistola, Fong Fu Hsu, Samar Muzaffar, Dianne M. Mueller, Stanley L. Hazen and Jay W. Heinecke

J. Biol. Chem. 1996, 271:19950-19956.
doi: 10.1074/jbc.271.33.19950